# Singular Points Analysis in Fingerprints Based on Topological Structure and Orientation Field

Jie Zhou[1], Jinwei Gu[1], and David Zhang[2]

[1] Department of Automation, Tsinghua University, Beijing 100084, China
jzhou@tsinghua.edu.cn
[2] Department of Computing, the Hong Kong Polytechnic University, Kowloon, Hong Kong

**Abstract.** As an important feature of fingerprints, singular points (including cores and deltas) not only represent the local ridge pattern characteristics, but also determine the topological structure (i.e. fingerprint type). In this paper, we have performed analysis for singular points in two aspects. (1) Based on the topology theory in 2D manifold, we deduced the relationship between cores and deltas in fingerprints. Specifically we proved that every completely captured fingerprint should have the same number of cores and deltas. We also proposed a flexible method to compute the Poincare Index for singular points. (2) We proposed a novel algorithm for singular point detection using global orientation field. After the initial detection with the widely-used Poincare Index method, the optimal singular points are selected to minimize the difference between the original orientation field and the model-based orientation field reconstructed from the singular points. The core-delta relation is used as a global constraint for final decision. Experimental results showed that our algorithm is rather accurate and robust.

## 1 Introduction

As a popular biometric feature, fingerprint is 2-dimensional oriented ridge-valley pattern captured from a finger by inked press, capacitive sensor, optical sensor, etc. Within each fingerprint, there are usually two kinds of singular points defined, i.e., *cores* and *deltas*, where the ridge orientation vanished or discontinued [1]. As an important topological feature for fingerprints, singular points can be used for fingerprint indexing [2], fingerprint alignment, orientation field modeling [3, 4], etc. In Fig. 1, singular points in different fingerprint types are provided.

Many previous works were proposed for singular point detection and analysis. Shu and Jain [5] used Partial Differential Equation modeling the local patterns for various kinds of singular points in general oriented texture images. For fingerprints, the Poincare Index is widely-used for singular points detection [2, 6, 7]. It is defined as the sum of the orientation change along a close circle around the points. Due to the noises in the real images, this local feature is not robust enough for detection. Tico et.al. [8] and Nilsson et.al.[9] used a multi-resolution approach to remove the spurious detections. Besides the above algorithms, there are also other approaches based on partitioning methods and heuristical rules for detection [10, 11].
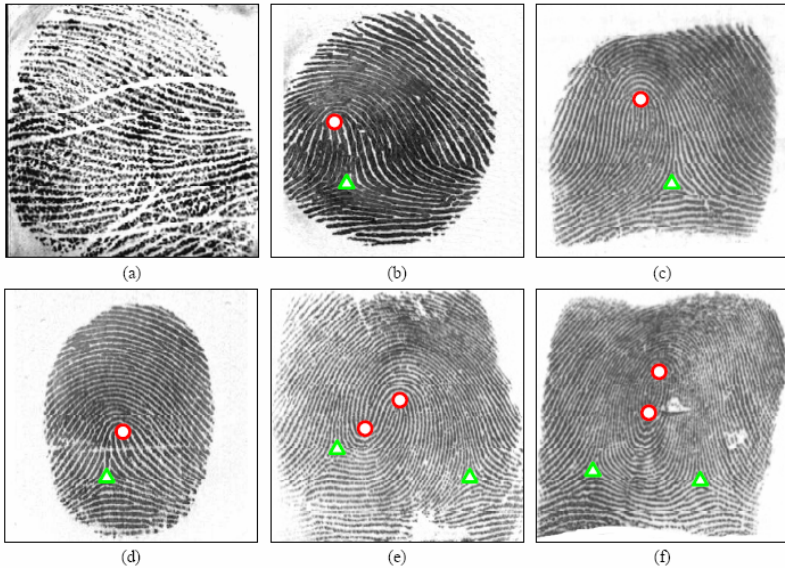
**Fig. 1.** Various types of fingerprints with the cores (circle) and the deltas (triangle) marked: (a) Plain Arch, (b) Tented Arch, (c) Left Loop, (d) Right Loop, (e) Twin Loop, and (f) Whorl

Basically all these works only utilized the local characteristics of singular points. However, only local information is not enough to discriminate the true singular points from spurious detections caused by creases, scars, smudges, damped prints, etc. In the orientation field, these spurious detections actually have nearly the same local patterns as the true ones. More global discriminative information should be incorporated for detection. One interesting work proposed by Perona [12] is orientation diffusion, which implicitly use the global constraint of the oriented texture during the dynamic diffusion process.

In this paper, we performed analysis of singular points based on topological structures and orientation field. It can be mainly summarized as the following two folds. (1) Based on the topology theory in 2D manifold, we deduced the relation between cores and deltas in fingerprints. Specifically we proved that every completely captured fingerprint should have the same number of cores and deltas. We also proposed a flexible method to compute the Poincare Index for singular points. Since the Poincare Index is independent with the integral paths if they are homotopic, we can adaptively select the path according to the confidence of the orientation values. (2) We proposed a novel algorithm for singular points detection using the orientation field. After the initial detection with the widely-used Poincare Index method, the optimal singular points are selected to minimize the difference between the original orientation field and the model-based orientation field reconstructed from the singular points. The core-delta relation is used as a global constraint for final decision. Experimental results showed that using both local feature and global information, our algorithm is rather accurate and robust for fingerprints with various qualities and types.

## 2   Topological Analysis for Fingerprint Structures

Given a continuous 2D vector field, $V(x, y)$, the Poincare Index for a path $\gamma$ is defined as follows:

$$I(\gamma) = \frac{1}{2\pi} \int_{(x,y)\in\gamma} d\phi(x, y),$$ (1)

where $\phi(x, y) = \arg\{V(x, y)\} \in [0, 2\pi)$, being the angle of point $(x; y)$ on $\gamma$. The integral is performed counterclockwise. The Poincare Index is an integer if the path $\gamma$ is closed. By computing I along a closed circle around a point $P$, we can define whether P is a singular point ($I \neq 0$) or not (I = 0). Refer [13, 14, 15] for more details.

Suppose $V$ is defined in a region, $\Omega$, with its exterior boundary, $\Gamma_E$, $\psi$ and its interior boundary, $\Gamma_I$ $\psi$, we denotes $\{\gamma_k\}$ as the singular points of $V$ inside $\Omega$ by the circles around them. C is an arbitrary closed path inside $\Omega$. There are two important properties about the Poincare Index formulated as follows:

**Property 1.** The Poincare Index of the boundary of a given region equals to the sum of the Poincare Indexes of the singular points inside this region, i.e.,

$$\sum I(\gamma_k) = I(\Gamma_E) - I(\Gamma_I)$$ (2)

**Property 2.** If two closed paths $\gamma$ and $\delta$ are homotopic, then

$$I(\gamma) = I(\delta).$$ (3)

That is to say, if there is no other singular points between $\gamma$ and $\delta$, their Poincare Indexes are the same. In Fig. 2, we can easily see that $I(C) = I(\Gamma_E)$.

For oriented texture images, such as fingerprints and fluid flow, it is natural to establish the connection with 2D topology theory. By computing the orientation field, $O$, we can build a vector field $V = \cos 2O + i \sin 2O$ [4, 6], and apply the above definitions and properties on these images. The singular points in fingerprints are found to be consistent with the singular points defined in topology.

An interesting conclusion for fingerprints can be deduced based on Property 1. Since fingerprints do not have interior boundary $\Gamma_I$, and only have isolated singular points (cores and deltas) with known Poincare index (+1 for core and -1 for delta), Eqn(2) is written as

$$N_c - N_d = I(\Gamma_E),$$ (4)

where $N_c$ is the number of the cores, $N_d$ is the number of the deltas.

If a fingerprint is captured completely, it can be assumed that the left, right, bottom, and top boundaries are nearly horizontal (see Fig. 1). Although different type fingerprints can vary inside, this assumption still holds for their boundaries. For the

path $\Gamma_E$ consisting of this kind of boundaries, $I(\Gamma_E) = 0$, and then $N_c = N_d$. Therefore, we concluded that, *for each completely captured fingerprint, there are the same numbers of cores and deltas.*
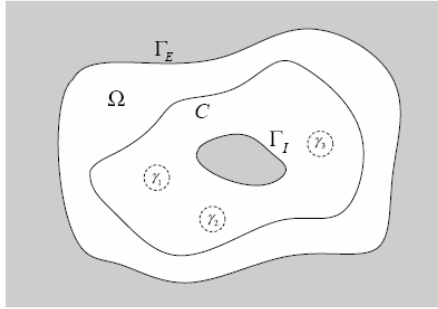


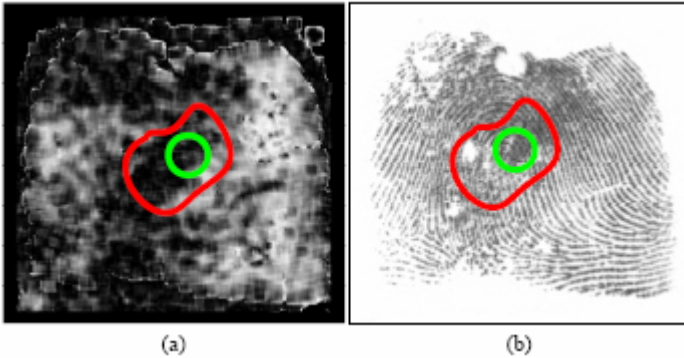**Fig. 2.** Illustration of Poincare index



**Fig. 3.** Adaptively choose the integral path for the Poincare Index Computation based on the homotopic property. (a) The con_dence of the orientation field [16]. (b) The selected optimal path (red) where the confidence is high and the conventional circle (green). The selected path can give the correct Poincare Index (I = 1) while the circle cannot (I = 0).

As for **Property 2**, we know that the Poincare Index can be computed along any closed path as long as it is homotopic with the closed circle around the point (i.e., not including any new singular point). This allows us to adaptively choose the integral path, for example, the path where the orientation confidence is high. An example is shown in Fig. 3.

In real applications, many fingerprint images are not complete. In this case, the number of cores is not necessarily equal to the number of deltas. Nevertheless, Eqn(4) still presents us a global topological constraint for singular points. Suppose the effective region of the fingerprints is $\Omega$, by computing $I(\partial\Omega)$, we can know that only finite combinations of the singular points are valid. In Table 1, we listed most of the

possible combinations of singular points for fingerprints with the Poincare Index and the possible types (PA-plain arch, TA-tented arch, LL-left loop, RL-right loop, TL-twin loop).

**Table 1.** Combinations of singular points with the Poincare Index and possible types

| $I(\partial\Omega)$ | Core | Delta | Possible Types |
|---|---|---|---|
| 0 | 0 | 0 | PA |
|  | 1 | 1 | LL, RL, TA |
|  | 2 | 2 | TL, Whorl |
| 1 | 1 | 0 | LL, RL, TA |
|  | 2 | 1 | TL, Whorl |
| 2 | 2 | 0 | TL, Whorl |

In Fig. 4, we listed two fingerprints along with the corresponding $I(\partial\Omega)$ and the singular points. The results verified our conclusion about the topological constraint about the singular points.
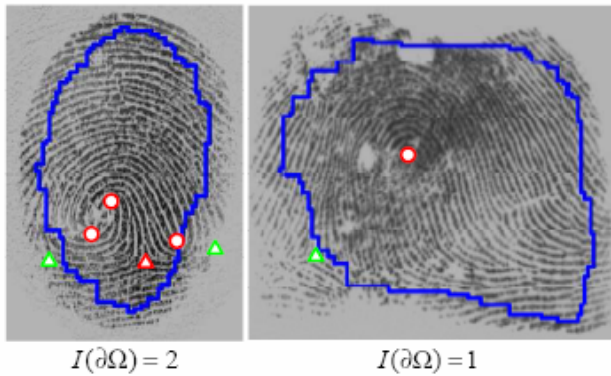


$I(\partial\Omega) = 2$          $I(\partial\Omega) = 1$

**Fig. 4.** Two examples for topological analysis of fingerprints. The blue curves are the boundary of the effective region. Circles are cores and triangles are deltas. The detected singular points are marked as red, while the singular points outside the boundary are marked with green.

## 3   Singular Points Detection Using Global Information

In this section, we proposed a novel algorithm for singular point detection using the global orientation field.

As known, singular points almost determine the global orientation field of fingerprints. In fact, there are several orientation field models related to singular points [3, 4, 19]. Our basic idea is to select the final optimal singular points by minimizing the difference between the original orientation field and the model-based orientation field reconstructed from the singular points. Specifically, each singular point detection is denoted by a triple, $(x, y, t)$, with its positions and type (core/delta). All singular

point candidates are in the set, $S = \{(x_i, y_i, t_i)\}_{i=1}^{M}$. The true singular points, s, is a subset of S. Denote the original orientation field with $O_0$, the reconstructed orientation field with $O(\Theta, s)$, where $\Theta$ is the model's parameter. The optimal singular points can be selected as:

$$s^* = \arg\min_{s \subseteq S} \|O_0 - O(\Theta, s)\|$$

where the difference function, $\|\cdot\|$, is defined as a averaged value of the absolute angular difference on all points of the fingerprint image.

Besides, the core-delta relation deduced in the above section can be used as a global constrain for the optimal singular points selection. By computing the global Poincare Index, we can remove some invalid combinations of singular points based on Table 1 and speed up the algorithm.
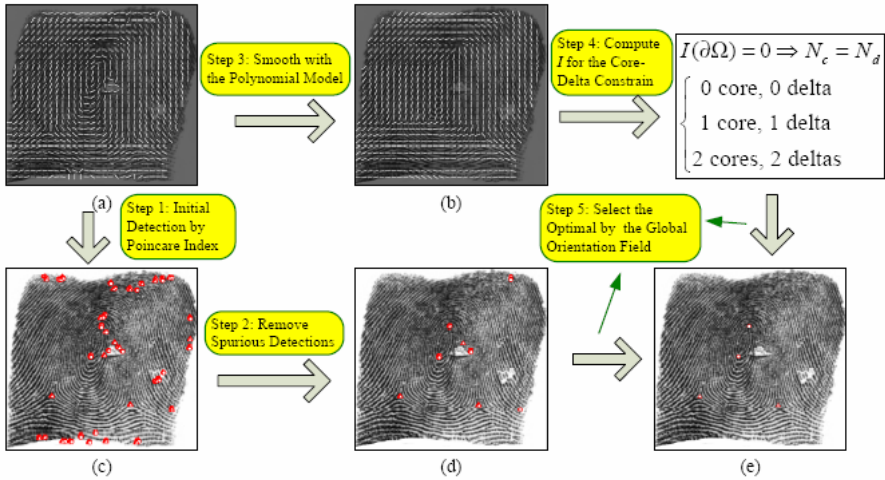


**Fig. 5.** Flowchart of our proposed detection method

Finally, we would like to emphasize that the widely-used Poincare Index method will not miss the true singular points as long as the process scale is low enough (i.e. small circle for computing), although it has lots of spurious detections. Actually this local method can detect the precise positions of the true singular points. This property guarantees our proposed method's robust and accurate performance after removing spurious detections. The flowchart of the proposed algorithm is shown in Fig. 5.

The original orientation field is computed by the hierarchical gradient-based method [17]. As for the model-based reconstructed orientation field, we choose the Zero-Pole model proposed by Sherlock and Monro in [3], considering both the model accuracy and the computational efficiency.

In this part, we propose to remove spurious points with a novel feature, $D$, which is a vector consisting the Differences of the ORIentation values along a Circle (DORIC)

around the point. For a given point $P$, we uniformly sampled a set of points, $T_1, T_2, \cdots, T_L$, along a circle around it in anticlockwise direction. The feature can be formulated as:

$$D(P) = [\partial O_1, \partial O_2, \cdots, \partial O_L]^T$$

where $O_i$ is the value of the orientation field, $O$ at the point $T_i$, $\partial O_i = O_{i+1} - O_i$. Fig. 6 showed three typical texture patterns and their DORIC feature plotted as curves. Since the orientation field $O$ is defined in $[0, \pi)$ instead of $[0, 2\pi)$, there will be a pulse for singular points (positive pulse for core, negative pulse for delta).
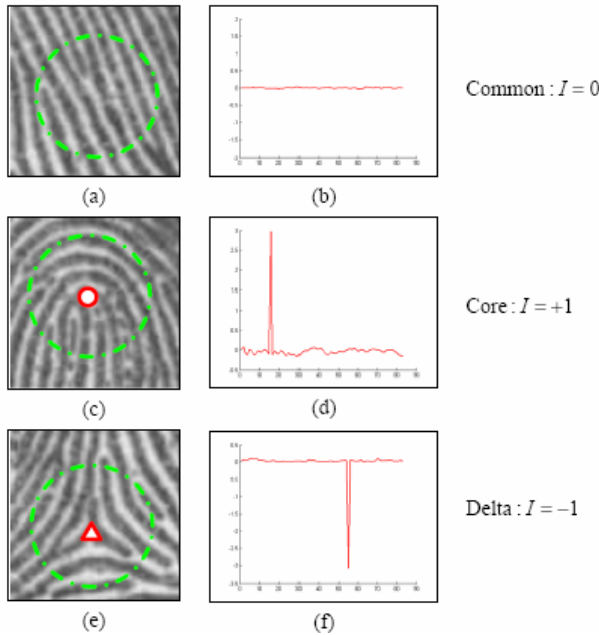


**Fig. 6.** Typical texture patterns and their DORIC features plotted as curves. There is a positive pulse for the core and a negative pulse for the delta.

This feature has strong relations with the Poincare Index defined in Eqn(1). Given a function $f(x)$ which equals to $x$ when $|x| < \pi/2$, $\pi - x$ when $x > \pi/2$, and $\pi + x$ when $x < -\pi/2$, it can be proved that $I = \frac{1}{\pi} \sum_{i=1}^{L} f(\partial O_i)$. DORIC contains more discriminative information than the Poincare Index. Fig. 7 showed two examples from a poor-quality fingerprint, which are falsely detected as core and delta by the Poincare Index but have very different DORIC features compared with true ones in Fig. 6.

For each point with non-zero Poincare Index, we compute its DORIC feature. If there is exactly one pulse with the height nearly up to $\pi$, it is a valid candidate

singular point; otherwise it will be removed from the candidate set $\mathcal{S}$. In practice, multiple DORIC features are computed along a set of circles at different scales around the point $P$. Based on the votes from these multiple-scale DORIC features, we made the decision whether it should be removed from the candidate set $\mathcal{S}$. The following experimental results proved that this feature can effectively remove spurious detections and can be computed very fast.
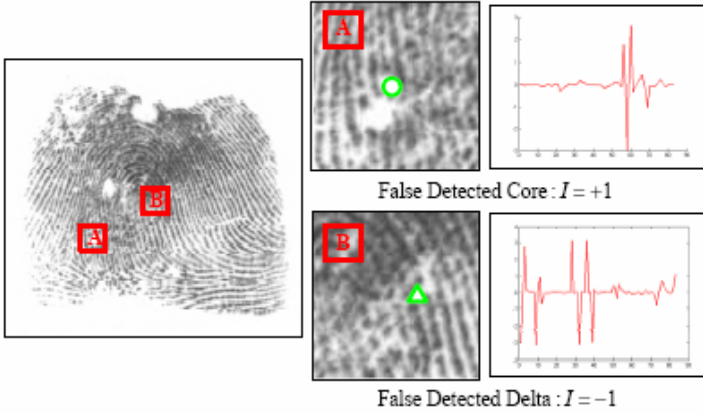


**Fig. 7.** Typical false detected examples by the Poincare Index, and their DORIC features plotted as curves. The features are different with those of the true singular points.

## 4   Experimental Results

The fingerprint database in our study consists of three parts. The first part contains 800 fingerprint images captured from 100 non-habituated cooperative subjects with a Digital Persona optical sensor, whose size is 512*320 pixels. The second part is a sample database from NIST Special Database 14 [20] that contains 40 inked fingerprint images. The image size is 480*512 pixels. The third part is from FVC2000 database (DB1, DB2, and DB3) [21] with 80*3 = 240 images captured by capacitive sensor and optical sensor. Thus there are total 1080 fingerprints in our database including various qualities and types.

In Fig. 8, we presented the detection results on some typical fingerprints which cover almost all the difficulties for singular point detection such as creases, scars, smudges, dryness, damped or blurred prints, etc. The first row showed the detected results with the widely-used Poincare Index method. The second row showed the results of our proposed method. Although we did not implement all of the previous methods using various heuristic rules or multiple resolutions, we would like to emphasize that, it is very hard to remove the spurious detections on these fingerprints without global constraints. With our method, the singular points are robustly detected and the positions are rather accurate.

To get the statistical performance of this algorithm, the singular points of these fingerprints are manually labeled by experts as the ground truth beforehand. The percentages for correct, missing, and false detection are provided in Table 2 (the position

distance threshold is defined as 5 pixels). We found that for most of the missing cases, it is usually that one or two deltas are not detected. Since the cores (if available) can be correctly detected, the detection results are still good for applications.
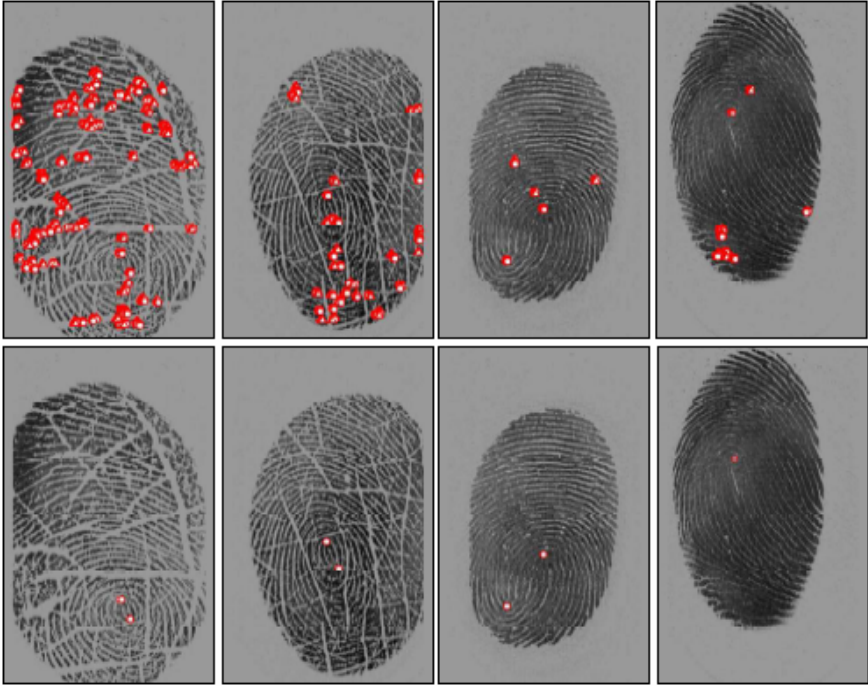


**Fig. 8.** Singular points detection results on various types of fingerprints. First row: results using widely-used Poincare Index method; second row: are based on our proposed method. These fingerprints cover most of the difficult situations for singular point detection: dryness, damped or blurred prints, and serious creases or scars.

Another advantage of our method is its real-time processing speed. It is currently implemented with Matlab and C on an AMD 2200Hz 512M PC computer without optimization. The average processing time for each fingerprint is around 0.10 sec.

**Table 2.** The performance of the proposed algorithm

|  | Correct | Missing | False Detection |
|---|---|---|---|
| Percentage | 80.6% | 14.6% | 4.8% |

## Acknowledgement

# References

1. Maltoni, D., Maio, D., Jain, A.K., Probhaker, S.: Handbook of Fingerprint Recognition. Springer, New York (2003)
2. Karu, K., Jain, A.K.: Fingerprint classification. Pattern Recognition 17(3), 389–404 (1996)
3. Sherlock, B., Monro, D.: A model for interpreting fingerprint topology. Pattern Recognition 26(7), 1047–1055 (1993)
4. Gu, J., Zhou, J.: A novel model for orientation field of fingerprints. In: IEEE Int. Conf. on Computer Vision and Pattern Recognition, vol. 2, pp. 493–498 (June 2003)
5. Shu, C.F., Jain, R.C.: Vector field analysis for oriented patterns. IEEE Trans. on Pattern Analysis and Machine Intelligence 16(9), 946–950 (1994)
6. Bazen, A.M.: Systematic methods for the computation of the directional fields and singular points of fingerprints. IEEE Trans. on Pattern Analysis and Machine Intelligence 24(7), 905–919 (2002)
7. Jain, A.K., Prabhakar, S., Hong, L.: A multichannel approach to fingerprint classification. IEEE Trans. On Pattern Analysis and Machine Intelligence 21(4), 348–359 (1999)
8. Tico, M., Kuosmanen, P.: A multiresolution method for singular points detection in fingerprint images. In: IEEE Int. Conf. on ISCAS, vol. 4, pp. 183–186 (July 1999)
9. Nilsson, K., Bigun, J.: Complex filters applied to fingerprint images detecting prominent symmetry points used for alignment. In: Tistarelli, M., Bigun, J., Jain, A.K. (eds.) ECCV 2002. LNCS, vol. 2359, pp. 39–47. Springer, Heidelberg (2002)
10. Ramo, P., Tico, M., Onnia, V., Saarinen, J.: Optimized singular point detection algorithm for fingerprint images. In: IEEE Int. Conf. on ICIP, vol. 3(3), pp. 242–245 (October 2001)
11. Cappelli, R., Lumini, A., Maio, D., Maltoni, D.: Fingerprint classification by directional image partitioning. IEEE Trans. on Pattern Analysis and Machine Intelligence 21(5), 402–421 (1999)
12. Perona, P.: Orientation diffusions. IEEE Trans. On Image Processing 7(3), 457–467 (1998)
13. Fulton, W.: Algebraic Topology: A First Course. Springer, New York (1995)
14. Scheuermann, G.: Topological Vector Field Visualization with Clifford Algebra. PhD thesis (January 1999)
15. Scheuermann, G., Kruger, H., Menzel, M., Rockwood, A.P.: Visualizing nonlinear vector field topology. IEEE Trans. on Visualization and Computer Graphics 4(2), 109–116 (1998)
16. Kass, M., Witkin, A.: Analyzing oriented pattern. Computer Vision, Graphics and Image Processing 37, 362–397 (1987)
17. Jain, A.K., Hong, L.: On-line fingerprint verification. IEEE Trans. on Pattern Analysis and Machine Intelligence 19(4), 302–314 (1997)
18. Zhou, J., Gu, J.: A model-based method for the computation of fingerprints' orientation field. IEEE Trans. on Image Processing 13(6), 821–835 (2004)
19. Zhou, J., Gu, J.: Modeling orientation fields of fingerprints with rational complex functions. Pattern Recognition 37(2), 389–391 (2004)
20. Sample of nist special database 14: Nist mated fingerprint card pairs (mfcp2). Available at http://www.nist.gov/srd/nistsd14.htm
21. Maio, D., Maltoni, D., Cappelli, R., Wayman, J.L., Jain, A.K.: Fvc2000: Fingerprint verification competition. IEEE Trans. on Pattern Analysis and Machine Intelligence 24(3), 402–412 (2002)